Published as: *Magn Reson Med*. 2019 April ; 81(4): 2238–2246.

Magneto-Caloric Materials as Switchable High Contrast Ratio MRI Labels

Mladen Barbic[1], **Stephen J. Dodd**[2], **H. Douglas Morris**[3], **Neil Dilley**[4], **Barbara Marcheschi**[5], **Alan Huston**[5], **Tim D. Harris**[1], and **Alan P. Koretsky**[2]

[1]Howard Hughes Medical Institute - Janelia Research Campus, Ashburn, VA, USA

[2]Laboratory of Functional and Molecular Imaging, NIH/NINDS, Bethesda, MD, USA

[3]NIH Mouse Imaging Facility, NIH/NINDS, Bethesda, MD, USA

[4]Quantum Design, San Diego, CA, USA

[5]US Naval Research Laboratory, Optical Sciences Division, Code 5611, Washington, DC, USA

Abstract

Purpose: To develop switchable and tunable labels with high contrast ratio for MRI using magneto-caloric materials that have sharp first order magnetic phase transitions at physiological temperatures and typical MRI magnetic field strengths.

Methods: A prototypical magneto-caloric material Iron-Rhodium (FeRh) was prepared by melt mixing, high-temperature annealing, and ice-water quenching. Temperature and magnetic field dependent magnetization measurements of wire-cut FeRh samples were performed on a vibrating sample magnetometer. Temperature-dependent MRI of FeRh samples was performed on a 4.7T MRI.

Results: Temperature-dependent MRI clearly demonstrated image contrast changes due to the sharp magnetic state transition of the FeRh samples in the MRI magnetic field (4.7T) and at a physiologically relevant temperature (~37°C).

Conclusion: A magneto-caloric material, FeRh, was demonstrated to act as a high contrast ratio switchable MRI contrast agent due to its sharp first order magnetic phase transition in the DC magnetic field of MRI and at physiologically relevant temperatures. A wide range of magneto-caloric materials are available that can be tuned by materials science techniques to optimize their response under MRI-appropriate conditions and be controllably switched in-situ with temperature, magnetic field, or a combination of both.

Keywords

MRI Labels; Magneto-Caloric Materials; Magnetic Particles

Correspondence: Mladen Barbic, Ph.D., Howard Hughes Medical Institute – Janelia Research Campus, Applied Physics and Instrumentation Group, 19700 Helix Drive, Ashburn, VA 20147 USA, barbicm@janelia.hhmi.org, Phone: 571-209-4127.

Introduction

Development of novel contrast mechanisms and labeling agents for MRI is important for further advancements in non-invasive cell imaging, tracking, and readout of physiological conditions in-vivo (1). There has been a large increase in utilizing conventional magnetic materials for preparation of nano- to micro- scale particle labels for MRI (2). Typically, this work uses bottom up chemical approaches to control composition and shape that may be useful for MRI sensing (3). In addition, some effort has gone into lithographic fabrication of more complex ferromagnetic micro-structures that have tunable spectroscopic properties (4) as well as sensing mechanisms that can be used to detect changes in the pH, ion concentration, temperature, or metabolism in the MRI settings (5).

Selection of appropriate magnetic materials for tunable labels in typical MRI settings of Tesla-scale DC magnetic fields and physiological temperatures of around 37°C is limited by the basic physical properties of most classical magnetic materials such as iron, iron oxides, manganese oxides and mixed metal formulations. Most magnetic materials have Curie temperatures in the hundreds of degrees Celsius, and therefore have a very flat saturation magnetization around physiological body temperatures of 37°C (310K). Moreover, standard MRI settings place these labels in large DC magnetic fields typically between 0.5–20 Tesla where all of these materials are magnetically saturated and therefore there is no way to make their net magnetic moment depend upon parameters such as temperature, pH, or other physiological parameters. It therefore remains a challenge to identify, design, or engineer unique magnetic materials that would have switchable and tunable properties with high differential contrast ratios in the MRI settings at physiological temperature where the DC magnetic fields are very large.

In this brief proof-of-concept report we put forward the case that there is a large class of materials, commonly known as Magneto-Caloric Materials (6, 7), whose magnetic properties provide a close match to the requirements for the design of high contrast ratio switchable and tunable MRI labels (8). More specifically, careful examination of the magneto-caloric materials' magnetic properties reveals that some of them have extremely sharp first-order magnetic phase transitions at typical physiological temperatures and in the presence of the large Tesla-scale magnetic fields typical of MRI settings. Furthermore, these sharp first-order magnetic phase transitions can have a positive or negative slope of magnetization vs. temperature, making them even stronger candidates as versatile materials for high differential contrast switchable MRI labels. Finally, magneto-caloric materials can be engineered and their magnetic properties fine-tuned through materials science techniques such as doping, alloying, thermal treatments and the like to optimize their response under physiological and MRI-appropriate conditions. As an example, we present the basic magneto-physical and MRI measurements on samples of Iron-Rhodium (FeRh), a proto-typical magneto-caloric material well-known and first extensively studied in the 1960s (9–16), in order to develop the case for and demonstrate the use of such materials for high differential contrast ratio MRI labels. This binary alloy (widely investigated for magnetic refrigeration (17), data storage (18), and spintronics (19, 20) applications) and other magneto-caloric materials have to our knowledge not been previously considered for switchable and tunable MRI labels.

Methods

Two sets of Iron-Rhodium granules (Fe 49% - Rh 51% atomic composition, of 99% and 99.9% nominal purity) were prepared by mixing in an arc melting furnace (American Elements Corporation Model FE-RH-02 and Model FE-RH-03, respectively), followed by a high-temperature anneal in Argon gas quartz tube furnace at 1,000°C for two weeks, and subsequently rapidly quenched in ice-water. This procedure typically results in the ordered body-centered-cubic (CsCl-type) crystal structure binary alloy FeRh with the bulk saturation magnetization of $M_S=1.3\times10^6$ A/m in the ferromagnetic state (9) (for comparison, pure Iron has bulk saturation magnetization of $M_S=1.7\times10^6$ A/m). FeRh samples were cut into mm-scale sample disks and buffed to a shiny metallic surface with an optical fiber polishing paper in order to remove any oxide from the samples. Temperature and field dependent magnetic measurements of the samples were then performed in a 9-Tesla Vibrating Sample Magnetometer (VSM, Quantum Design, Inc.). In order to demonstrate the basic proof-of-concept feasibility of a magneto-caloric material as a tunable and switchable high differential contrast agent at physiological temperatures and typical MRI settings, a 4.7 Tesla MRI scanner (Bruker Biospin, Inc.) was used. This choice was made because the available MRI polarizing magnetic field of that scanner was closest to the value where the sharp first order magnetic phase transition happens near the physiological temperature of 37°C (310°K). For the MRI demonstration, the sample was embedded in agarose next to a MRI-compatible optical fiber-based thermometer (FISO Technologies, Inc.). The sample container was wrapped in tubing connected to a temperature controlled water circulating bath (Model Cole-Parmer Polystat Standard 3–6L Heat/Cool Bath) in order to sweep and control the temperature of the sample and its environment around physiologically relevant temperature range (10–55°C).

Results

Figures 1a and 1b show the VSM measurements of the magnetic moment of the FeRh samples as a function of temperature at different constant magnetic fields. Both samples exhibited a sharp first order magnetic transition from an antiferromagnetic to a ferromagnetic state over a very narrow range of physiologically relevant temperatures. More specifically, the 99% purity FeRh sample has a sharp magnetic phase transition around room and body temperatures (27°C=300K and 37°C = 310K, respectively) at the constant magnetic field of around 1 Tesla, while the 99.9% purity FeRh sample has a sharp magnetic phase transition around room and body temperatures at the constant magnetic field of around 5 Tesla. These results are in line with the previously reported measurements of FeRh (9), and demonstrate several important features. The most important one is that the magnetization of FeRh changes through the transition by a factor of about twenty in absolute value, and it does so over a very narrow temperature range around the physiological body temperature and in the presence of a large Tesla-scale magnetic field. The second important feature is that the temperature dependence and magnetic properties of FeRh (and magneto-caloric materials in general) are highly dependent on sample purity (14). Conversely, this demonstrates the attractive feature of FeRh (and other magneto-caloric materials) that, through careful materials science preparation and process control of impurities and crystal structure, one can tune and engineer FeRh to have a sharp magnetic phase transition at the

desired temperature and bias magnetic field (12, 14, 21, 22) at physiological body temperatures and magnetic field strength of the MRI used. Furthermore, such temperature dependence of magnetization demonstrates that, once the proper magneto-caloric material is prepared for a specific magnetic field of the MRI used, the magnetization of that magneto-caloric label can in principle be switched in-situ by modest temperature changes on the order of a few degrees Celsius.

In the second set of VSM magnetic measurements, shown in Figures 2a and 2b, the magnetic moments of the two FeRh disk samples of different purity are measured as a function of the varying magnetic field at constant temperatures (room temperature of 27°C=300K and physiological body temperature of 37°C = 310K, respectively). The sharp magnetic phase transition with varying magnetic field is again present at large magnetic field values. Specifically, the 99% purity FeRh sample has a sharp magnetic phase transition around room and body temperatures at the magnetic field values between 0.5–2 Tesla, while the 99.9% purity FeRh sample has a sharp magnetic phase transition around room and body temperatures at the magnetic field values between 4–6 Tesla. These results are also in line with the previously reported measurements of magnetization vs. magnetic field for FeRh (13, 15, 23), and demonstrate another important feature that, once the proper magneto-caloric material is fabricated as a switchable MRI label for the specific magnetic field of the MRI used, the magnetization of that magneto-caloric label can in principle be switched in-situ with additionally added or subtracted magnetic field or by temporarily removing the sample from the MRI bore.

Measurements described in Figures 1 and 2 guided the experimental choices for demonstrating the basic proof-of-concept feasibility of a magneto-caloric FeRh material as a switchable high differential contrast MRI agent. Of the two samples that we prepared, 99.9% purity FeRh sample displayed a sharper first order magnetic transition at a higher bias DC magnetic field (of around 5 Tesla) at the physiological temperature of 37°C. These parameters narrowed our available scanner choices to a 4.7 Tesla MRI (Bruker Biospin, Inc.). Figures 3(a-f) show six representative gradient-echo images (out of 52) of the effect of the mm-scale disk of FeRh on the surrounding agarose (Image parameters: TR/TE = 100/2.2 ms, FA = 25 degrees, nominal resolution = 0.46 × 0.46 × 1mm, FOV = 60.0 × 60.0 mm) as the temperature of the set-up (diagrammatically shown in Figure 3g) is swept through physiologically relevant temperature range (10–55°C) at the constant MRI magnetic field of 4.7 Tesla. The clearly demonstrated agarose image phase shift with concomitant magnetic field change emanating from the magneto-caloric FeRh sample is seen in the increase in size of the MRI signal void in the magnitude images produced around the sample in Figures 3(a-f). As the 99.9 % purity FeRh sample magnetization data of Figure 1b dictates, the temperature increase drives the sample to transition from the low-moment antiferromagnetic phase below the transition temperature to the high-moment ferromagnetic phase above the transition temperature and then back to the low-moment antiferromagnetic phase as the sample is cooled. Loss of signal in the MRI of Figure 3(a-f) due to the changing magnetic moment of the magneto-caloric material closely follows the magnetic properties shown in Figure 1b. The size of the region with signal dropout due to the high magnetic field gradients associated with the FeRh approximately doubles in each dimension leading to a factor of 8

in volume. This is plotted in Figure 3(h) which shows the MRI signal loss region size (in a linear dimension) as a function of temperature.

We note that in our prototypical magneto-caloric material (FeRh), the magnetic moment of such MRI label is minimal or essentially zero in the initial lower temperature range when translated through a high magnetic field gradient of the scanner bore, and only becomes magnetic in the elevated temperature range while already inside the MRI scanner at a uniform DC magnetic field of the scanner bore. Therefore, we do not expect and we did not detect in our experiments any problems of motion when the material in agarose goes through its sharp magnetic phase transition.

Discussion

In this report Iron-Rhodium (FeRh) is demonstrated to be useful as a high differential contrast ratio MRI agent that is switchable and tunable in typical MRI settings (Tesla-scale magnetic fields) and in-vivo physiological temperatures (around 37°C) based on a very sharp, first order magnetic phase transition. It is important to emphasize that Iron-Rhodium is only one in a large repertoire of magneto-caloric materials that have similar switching characteristics under similar environmental conditions, where sharp first order magnetic phase transition with a positive M vs. T slope is observed at physiological temperatures and Tesla-scale magnetic fields (24–29). Furthermore, there are many magneto-caloric materials where the sharp first-order magnetic phase transitions can also have a negative M vs. T slope at physiological temperatures and Tesla-scale fields (30–34), or even a combination of sharp positive and negative slopes (35, 36), making magneto-caloric compounds even stronger candidates as versatile materials for high differential contrast switchable MRI labels. Careful review of these reports indicates that the negative slope is just as sharp and the change in magnetization just as large as we present for the positive slope in our report for FeRh.

There are a number of ways that causing the magnetic transition in a magneto-caloric material can occur in addition to control of temperature of the entire sample. In this proof-of-concept report the FeRh switchable MRI contrast agent was reversibly switched by thermal cycling of the entire sample set-up over the physiologically relevant temperature range. Other potential engineering solutions to magneto-caloric MRI label switching include heating by MRI compatible focused ultrasound (37), high-frequency inductive heating (38) and cooling (39) or label switching by adding or subtracting to the main magnetic field of the MR. In the simplest version this can be accomplished by temporarily removing the sample from the MRI bore or changing the magnetic field using well established field cycling techniques (40).

The magneto-thermal properties of the magneto-caloric materials are important for making a switchable MRI sensor. Most important is crafting the materials so that the location of the first order magnetic phase transition of the label is in a relevant regime. Figure 4 schematically describes specific examples. In Figure 4(a) the MRI label has two stable magnetic states (indicated by the solid black dots) at 37°C (310K). This example is well represented by our 99.9% purity FeRh sample at 5 Tesla, as shown in Figure 1(b). In the low magnetic moment state the label has a small impact on MRI signal and is referred to as the

Label OFF state. The Label ON state can be switched by temporarily raising the materials' temperature by a few degrees C (approximately ΔT=5°C for our 99.9% purity FeRh sample at 5 Tesla shown in Figure 1(b) through application of a heating pulse using any relevant method of global or localized heating. Once the label has equilibrated to the equilibrium temperature of 37°C, it remains in the high magnetic moment state and now has a much larger effect on MRI signal (Label ON). It can be switched off again by active cooling where the label temperature is temporarily lowered. Once the label relaxes back to the equilibrium temperature of 37°C, it will be in the low magnetic moment state and again MRI invisible (Label OFF). This is exactly the procedure performed in this work on our FeRh sample as described in Figure 3.

The second possibility for modulating the label state is described in Figure 4(b). In this case the MRI label has only one stable magnetic state (indicated by the solid black dot) at 37°C (310K). This example is well represented by our 99.9% purity FeRh sample at 3 Tesla, as shown in Figure 1(b). This is the low magnetic moment Label OFF state. The Label state can be temporarily switched to ON by raising its temperature through application of a larger heat pulse than was described in Figure 4(a) since higher temperature change is required to take the sample through the first order magnetic phase transition (In the case of our 99.9 % purity FeRh at 3T as shown in Figure 1(b), it would take approximately ΔT=20°C to switch the label). The Label ON state remains in the high magnetic moment state as long as the label temperature is above the phase transition temperature. As the label thermally relaxes back to the equilibrium temperature of 37°C, it automatically goes back through the phase transition into a low magnetic moment state and switches to the Label OFF state. The advantage of this configuration is that active cooling is not required for switching the label into the Label OFF state, but the disadvantage is that the higher temperature increase is required to temporarily switch the label into the MRI visible ON state. Proper matching of the material to the MRI magnetic field used should allow this temperature change to be minimized to some extent.

Another feature of MRI switchable labels brought about by the variety of magneto-thermal properties of magneto-caloric materials is the possibility of multiplexed labels made to go from Label OFF to Label ON at different magnetic field or temperature values by appropriate materials science design. Figure 4(c) describes the possibility of two switchable MRI labels that can be differentiated in images from MRI scanners operating at different magnetic field values. Label 1 has a first order magnetic phase transition at 2 Tesla and is well represented by our 99% purity FeRh sample at 27°C (300K) shown in Figure 2 (a). Label 2 has a first order magnetic phase transition at 6 Tesla and is well represented by our 99.9% purity FeRh sample at 27°C (300K) shown in Figure 2(b). In a 1T MRI scanner, both of these labels would be in the low magnetic moment state below their respective first order magnetic phase transition temperatures and therefore in the Label OFF state. In a 4T MRI scanner, Label 1 would be in the high magnetic moment state above its magnetic phase transition temperature and therefore Label 1 ON, while Label 2 would still be in the low magnetic moment state below its magnetic phase transition temperature and therefore Label 2 OFF. Finally, in a 7T MRI scanner, both of these labels would be in the high magnetic moment states above their respective magnetic phase transition temperatures and therefore

MRI visible (both Labels 1 and 2 ON). Images from these MRI scanners with different operating DC magnetic fields would readily differentiate the two labels.

A major limitation at the present time is that most demonstrations of magneto-caloric materials at present are done on mm scale materials, as was used for this report. This scale label may have interesting applications for use in implantable devices on interventional settings. However, it will be important to work out fabrication techniques that will allow sub-micron materials to be made for most biological applications. Progress in preparing high quality magneto-caloric materials in micro-scale and nano-scale thin film and particle form has been rapid and significant, and the available knowhow in precisely tuning their magneto-thermal properties through vacuum and solution-based synthesis, doping, alloying, and thermal and mechanical treatment is by now extensive (41–52). Review of these reports also indicates that the properties of FeRh (and magneto-caloric materials in general) in micro-thin film and micro-particle forms often (but not always) maintain magnetic properties similar to the bulk sample form used in our report. Designing the necessary custom MRI-compatible focused ultrasound or inductive heating, thermo-electric cooling, and magnetic field instrumentation for controlled switching of these high differential contrast MRI agents for in-vivo applications is certainly within reach.

It is interesting to compare the roughly 10-fold change in moment that occurs over a five degrees C temperature range in the Fe-Rh sample to other materials that have been used as temperature sensors in NMR and MRI. The chemical shift of water has been used and varies about 0.01 PPM/deg C which at 4.7T is about 2 Hz per degree (53). Dysprosium chelates (Dy-EDTA) shifts about 0.09 PPM/deg C (54). This is nine times larger than water or about 18 Hz per degree. The frequency shift related to the magneto-caloric material will depend on the distance from the material (Fig 3). An estimate of the frequency shift from our sample is that there was approximately 500 Hz per degree at 10 diameters from the particle in our FeRh magnetocaloric material. Water and Dy-EDTA are linear over a large temperature range while the magnetocaloric material is very non-linear and only effective at measuring temperature over a narrow range. Nonetheless the large moment shifts with temperature may make it a useful temperature sensor for some applications. Other approaches have used compounds/mixtures which exhibit non-linear phase transitions at specific temperatures and have been proposed as MRI sensing agents (55)- (56).

We note that the temperature (or magnetic field) changes the magnetic moment of the particle, and thus all label contrast effects are on B_0 field which can be measured using T2* or other more quantitative field mapping strategies. The important advantage is that an image can be acquired in the low magnetic moment state and in the high magnetic moment state (or vice versa) which allows subtraction of all the artifacts that can be associated with T2* images. Unfortunately, we do not presently see a way to use the change in moment directly to produce a T1 agent from these particles. It may be that water exchange with the surface of the particle will have some T1 relaxation effect as is the case with iron oxide particles.

We envision first applications will be in pre-clinical imaging and possible for interventional applications, for example as part of catheters. This will allow us to work with larger

materials, control temperature over broad ranges, and eliminate safety and toxicity concerns in future proof of concept studies. We are in process of making small enough magneto-caloric MRI label particles that will require us to also investigate the issue related to particle circulation and coagulation. Likely these issues will be dominated by the surface coating as is the case with other MRI particle formulations. Considering the magnetic moment values we see in our initial proof-of-concept demonstration, we expect to be able to detect individual micron sized particles and address the coating issues as is now routinely done with iron oxides. This will be very important should such particles be potentially used by injecting into the circulatory system and targeting to specific tissues as would be required in Magnetic Resonance guided Focused Ultrasound applications (57, 58).

In conclusion the usefulness of magneto-caloric materials as potential switchable contrast for MRI has been demonstrated. The sharp phase transition due to small changes in temperature or magnetic field leading to order of magnitude changes in magnetic moment offer exciting possibilities for development of novel sensors for MRI.

Acknowledgments

This research was supported by the Howard Hughes Medical Institute and the NINDS Intramural Research Program of the National Institutes of Health. We thank Michael Wagner of the George Washington University and Hatem ElBidweihy of the United States Naval Academy for the initial help in magnetometry, Virgil Provenzano of the National Institute of Standards and Technology (NIST) for the discussions on the magneto-caloric materials properties, Bruce Bowers of HHMI-Janelia Research Campus for wire cutting of our FeRh samples, and Marty Lizak of the Mouse Imaging Facility, NIH for assistance on the 4.7T Bruker MRI.

References

1. Ahrens ET, Bulte JW. Tracking immune cells in vivo using magnetic resonance imaging. Nat Rev Immunol. 2013;13(10):755–63. [PubMed: 24013185]
2. Shapiro EM, Skrtic S, Sharer K, Hill JM, Dunbar CE, Koretsky AP. MRI detection of single particles for cellular imaging. Proc Natl Acad Sci U S A. 2004;101(30):10901–6. [PubMed: 15256592]
3. Bulte JWM, Kraitchman DL. Iron oxide MR contrast agents for molecular and cellular imaging. Nmr Biomed. 2004;17(7):484–99. [PubMed: 15526347]
4. Zabow G, Dodd S, Moreland J, Koretsky A. Micro-engineered local field control for high-sensitivity multispectral MRI. Nature. 2008;453(7198):1058–63. [PubMed: 18563157]
5. Zabow G, Dodd SJ, Koretsky AP. Shape-changing magnetic assemblies as high-sensitivity NMR-readable nanoprobes. Nature. 2015;520(7545):73–7. [PubMed: 25778701]
6. Franco V, Blazquez JS, Ingale B, Conde A. The Magnetocaloric Effect and Magnetic Refrigeration Near Room Temperature: Materials and Models. Annu Rev Mater Res. 2012;42:305–42.
7. Moya X, Kar-Narayan S, Mathur ND. Caloric materials near ferroic phase transitions. Nat Mater. 2014;13(5):439–50. [PubMed: 24751772]
8. Barbic M, Harris TD, Dodd S, Morris HD, Koretsky AP, Marcheschi B, Huston A, and Dilley NR, Magneto-Caloric Materials as Tunable and Switchable Labels for MRI. Proc. Intl. Soc. Mag. Reson. Med 25 (2017) 0999, 25th Annual Meeting of ISMRM; 2017; Honolulu, HI, USA.
9. Kouvel JS, Hartelius CC. Anomalous Magnetic Moments and Transformations in Ordered Alloy Ferh. J Appl Phys. 1962;33(3):1343-&.
10. Shirane G, Chen CW, Nathans R, Flinn PA. Hyperfine Fields and Magnetic Moments in Fe-Rh System. J Appl Phys. 1963;34(4):1044-&.
11. Shirane G, Nathans R, Chen CW. Magnetic Moments + Unpaired Spin Densities in Fe-Rh Alloys. Phys Rev. 1964;134(6a):1547-+.

12. Walter PHL. Exchange Inversion in Ternary Modifications of Iron Rhodium. J Appl Phys. 1964;35(3p2):938-&.
13. Zakharov AI, Kadomtseva AM, Levitin RZ, Ponyatovskii EG. Magnetic and Magnetoelastic Properties of a Metamagnetic Iron-Rhodium Alloy. Sov Phys Jetp-Ussr. 1964;19(6):1348–53.
14. Kouvel JS. Unusual Nature of Abrupt Magnetic Transition in Ferh and Its Pseudobinary Variants. J Appl Phys. 1966;37(3):1257-&.
15. Levitin RZ, Ponomare Bk Magnetostriction of Metamagnetic Iron-Rhodium Alloy. Sov Phys Jetp-Ussr. 1966;23(6):984-&.
16. Lommel JM. Magnetic and Electrical Properties of Ferh Thin Films. J Appl Phys. 1966;37(3): 1483-&.
17. Annaorazov MP, Asatryan KA, Myalikgulyev G, Nikitin SA, Tishin AM, Tyurin AL. Alloys of the Fe-Rh System as a New Class of Working Material for Magnetic Refrigerators. Cryogenics. 1992;32(10):867–72.
18. Thiele JU, Maat S, Fullerton EE. FeRh/FePt exchange spring films for thermally assisted magnetic recording media. Appl Phys Lett. 2003;82(17):2859–61.
19. Marti X, Fina I, Frontera C, Liu J, Wadley P, He Q, et al. Room-temperature antiferromagnetic memory resistor. Nat Mater. 2014;13(4):367–74. [PubMed: 24464243]
20. Moriyama T, Matsuzaki N, Kim KJ, Suzuki I, Taniyama T, Ono T. Sequential write-read operations in FeRh antiferromagnetic memory. Appl Phys Lett. 2015;107(12).
21. Nishimura K, Nakazawa Y, Li L, Mori K. Magnetocaloric effect of Fe(Rh1-xPdx) alloys. Mater Trans. 2008;49(8):1753–6.
22. Barua R, Jimenez-Villacorta F, Lewis LH. Towards tailoring the magnetocaloric response in FeRh-based ternary compounds. J Appl Phys. 2014;115(17).
23. Mckinnon JB, Melville D, Lee EW. Antiferromagnetic-Ferromagnetic Transition in Iron-Rhodium Alloys. J Phys Part C Solid. 1970;3(1):S46-+.
24. Swoboda TJ, Cloud WH, Bither TA, Sadler MS, Jarrett HS. Evidence for an Antiferromagnetic-Ferrimagnetic Transition in Cr-Modified Mn2sb. Phys Rev Lett. 1960;4(10):509–11.
25. Kainuma R, Imano Y, Ito W, Sutou Y, Morito H, Okamoto S, et al. Magnetic-field-induced shape recovery by reverse phase transformation. Nature. 2006;439(7079):957–60. [PubMed: 16495995]
26. Ito W, Nagasako M, Umetsu RY, Kainuma R, Kanomata T, Ishida K. Atomic ordering and magnetic properties in the Ni45Co5Mn36.7In13.3 metamagnetic shape memory alloy. Appl Phys Lett. 2008;93(23).
27. Liu J, Scheerbaum N, Lyubina J, Gutfleisch O. Reversibility of magnetostructural transition and associated magnetocaloric effect in Ni-Mn-In-Co. Appl Phys Lett. 2008;93(10).
28. Bourgault D, Tillier J, Courtois P, Maillard D, Chaud X. Large inverse magnetocaloric effect in Ni45Co5Mn37.5In12.5 single crystal above 300 K. Appl Phys Lett. 2010;96(13).
29. Liu J, Gottschall T, Skokov KP, Moore JD, Gutfleisch O. Giant magnetocaloric effect driven by structural transitions. Nat Mater. 2012;11(7):620–6. [PubMed: 22635044]
30. Wada H, Tanabe Y. Giant magnetocaloric effect of MnAs1-xSbx. Appl Phys Lett. 2001;79(20): 3302–4.
31. Tegus O, Bruck E, Buschow KHJ, de Boer FR. Transition-metal-based magnetic refrigerants for room-temperature applications. Nature. 2002;415(6868):150–2. [PubMed: 11805828]
32. Pasquale M, Sasso CP, Lewis LH, Giudici L, Lograsso T, Schlagel D. Magnetostructural transition and magnetocaloric effect in Ni55Mn20Ga25 single crystals. Phys Rev B. 2005;72(9).
33. Caron L, Ou ZQ, Nguyen TT, Thanh DTC, Tegus O, Bruck E. On the determination of the magnetic entropy change in materials with first-order transitions. J Magn Magn Mater. 2009;321(21):3559–66.
34. Liu EK, Wang WH, Feng L, Zhu W, Li GJ, Chen JL, et al. Stable magnetostructural coupling with tunable magnetoresponsive effects in hexagonal ferromagnets. Nat Commun. 2012;3.
35. Krenke T, Duman E, Acet M, Wassermann EF, Moya X, Manosa L, et al. Inverse magnetocaloric effect in ferromagnetic Ni-Mn-Sn alloys. Nat Mater. 2005;4(6):450–4. [PubMed: 15895096]

36. Aksoy S, Krenke T, Acet M, Wassermann EF, Moya X, Manosa L, et al. Tailoring magnetic and magnetocaloric properties of martensitic transitions in ferromagnetic Heusler alloys. Appl Phys Lett. 2007;91(24).
37. Chopra R, Curiel L, Staruch R, Morrison L, Hynynen K. An MRI-compatible system for focused ultrasound experiments in small animal models. Med Phys. 2009;36(5):1867–74. [PubMed: 19544806]
38. Zhang Q, Chung YC, Lewin JS, Duerk JL. A method for simultaneous RF ablation and MRI. Jmri-J Magn Reson Im. 1998;8(1):110–4.
39. McAllen RM, Farrell M, Johnson JM, Trevaks D, Cole L, McKinley MJ, et al. Human medullary responses to cooling and rewarming the skin: A functional MRI study. P Natl Acad Sci USA. 2006;103(3):809–13.
40. Alford JK, Scholl TJ, Handler WB, Chronik BA. Design and Construction of a Prototype High-Power B-0 Insert Coil for Field-Cycled Imaging in Superconducting MRI Systems. Concept Magn Reson B. 2009;35b(1):1–10.
41. Lommel JM, Kouvel JS. Effects of Mechanical and Thermal Treatment on Structure and Magnetic Transitions in Ferh. J Appl Phys. 1967;38(3):1263-&.
42. Takahashi M, Oshima R. Annealing Effect on Phase-Transition of Equiatomic Ferh Alloy. Mater T Jim. 1995;36(6):735–42.
43. Marquina C, Ibarra MR, Algarabel PA, Hernando A, Crespo P, Agudo P, et al. Magnetic and magnetoelastic behavior of mechanically alloyed FeRh compound. J Appl Phys. 1997;81(5):2315–20.
44. Cao JW, Nam NT, Inoue S, Ko HYY, Phuoc NN, Suzuki T. Magnetization behaviors for FeRh single crystal thin films. J Appl Phys. 2008;103(7).
45. Ding Y, Arena DA, Dvorak J, Ali M, Kinane CJ, Marrows CH, et al. Bulk and near-surface magnetic properties of FeRh thin films. J Appl Phys. 2008;103(7).
46. Jia Z, Harrell JW, Misra RDK. Synthesis and magnetic properties of self-assembled FeRh nanoparticles. Appl Phys Lett. 2008;93(2).
47. Ko HYY, Suzuki T, Nam NT, Phuoc NN, Cao J, Hirotsu Y. Magnetic and structural characterizations on nanoparticles of FePt, FeRh and their composites. J Magn Magn Mater. 2008;320(22):3120–3.
48. Suzuki I, Koike T, Itoh M, Taniyama T, Sato T. Stability of ferromagnetic state of epitaxially grown ordered FeRh thin films. J Appl Phys. 2009;105(7).
49. Baldasseroni C, Bordel C, Gray AX, Kaiser AM, Kronast F, Herrero-Albillos J, et al. Temperature-driven nucleation of ferromagnetic domains in FeRh thin films. Appl Phys Lett. 2012;100(26).
50. Han GC, Qiu JJ, Yap QJ, Luo P, Laughlin DE, Zhu JG, et al. Magnetic stability of ultrathin FeRh films. J Appl Phys. 2013;113(17).
51. Zhou TJ, Cher MK, Shen L, Hu JF, Yuan ZM. On the origin of giant magnetocaloric effect and thermal hysteresis in multifunctional alpha-FeRh thin films. Phys Lett A. 2013;377(42):3052–9.
52. Suzuki I, Hamasaki Y, Itoh M, Taniyama T. Controllable exchange bias in Fe/metamagnetic FeRh bilayers. Appl Phys Lett. 2014;105(17).
53. Soher BJ, Wyatt C, Reeder SB, MacFall JR. Noninvasive Temperature Mapping With MRI Using Chemical Shift Water-Fat Separation. Magn Reson Med. 2010;63(5):1238–46. [PubMed: 20432295]
54. Shapiro EM, Borthakur A, Shapiro MJ, Reddy R, Leigh JS. Fast MRI of RF heating via phase difference mapping. Magn Reson Med. 2002;47(3):492–8. [PubMed: 11870836]
55. Venkataramani S, Jana U, Dommaschk M, Sonnichsen FD, Tuczek F, Herges R. Magnetic Bistability of Molecules in Homogeneous Solution at Room Temperature. Science. 2011;331(6016):445–8. [PubMed: 21273483]
56. Muller RN, Vander Elst L, Laurent S. Spin transition molecular materials: Intelligent contrast agents for magnetic resonance imaging. J Am Chem Soc. 2003;125(27):8405–7. [PubMed: 12837114]
57. Chang WS, Jung HH, Zadicario E, Rachmilevitch I, Tlusty T, Vitek S, et al. Factors associated with successful magnetic resonance guided focused ultrasound treatment: efficiency of acoustic energy delivery through the skull. J Neurosurg. 2016;124(2):411–6. [PubMed: 26361280]

58. Chen L, Cvetkovic D, Wang B, Gupta R, Ma CMC. Management of Prostate Cancer Using Magnetic Resonance Guided Pulsed Focused Ultrasound-Mediated Targeted Chemotherapeutic Agent Delivery. Int J Radiat Oncol. 2016;96(2):E260–E.

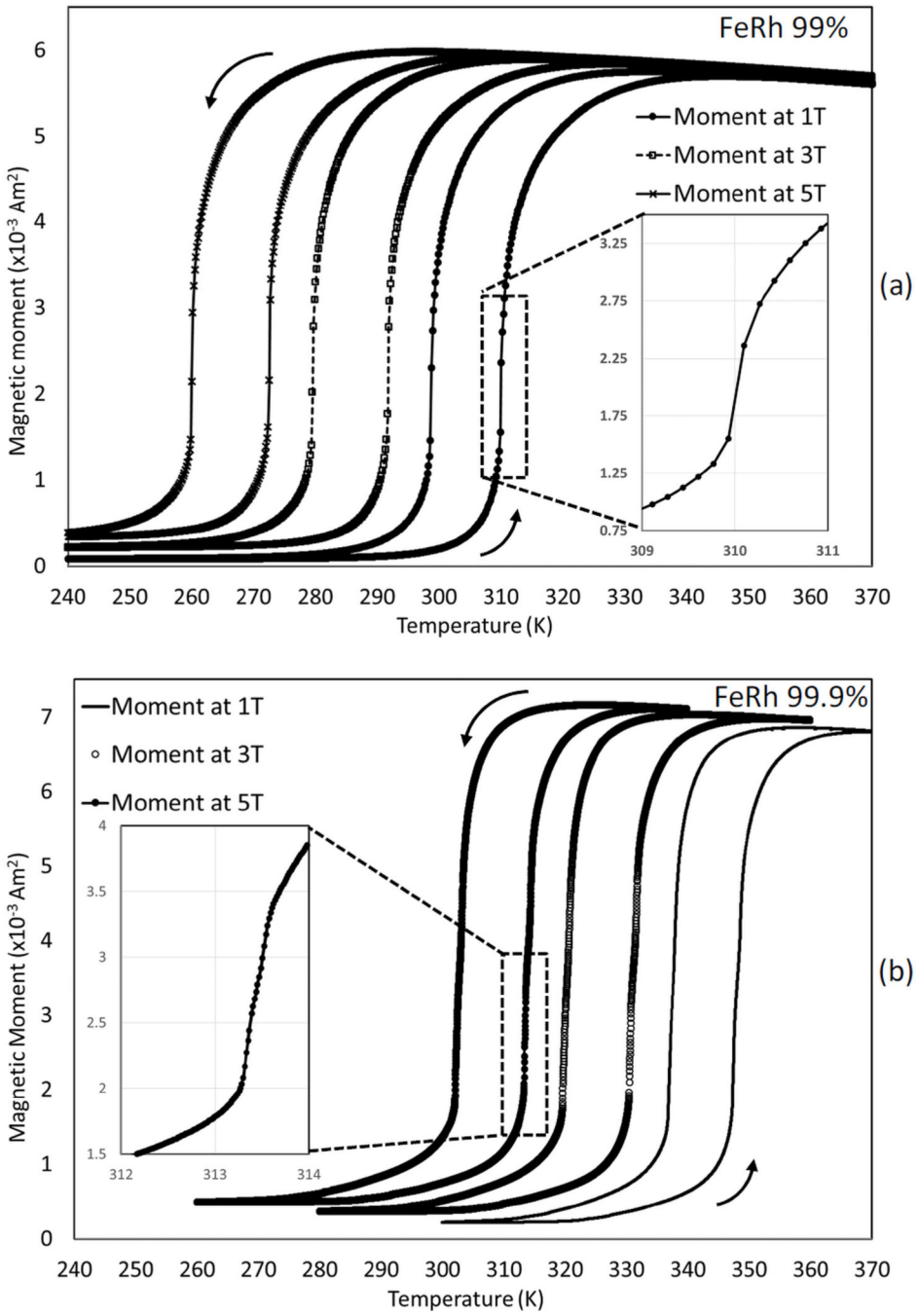

Figure 1.

VSM measurement of Magnetic Moment vs. Temperature of (a) 99% purity Iron-Rhodium (FeRh) disk sample at 1T, 3T and 5T and (b) 99.9% purity FeRh disk sample at 1T, 3T, and 5T. Insets in both figures show expanded M vs. T data in the range where the magnetization changes most rapidly at physiological temperatures.

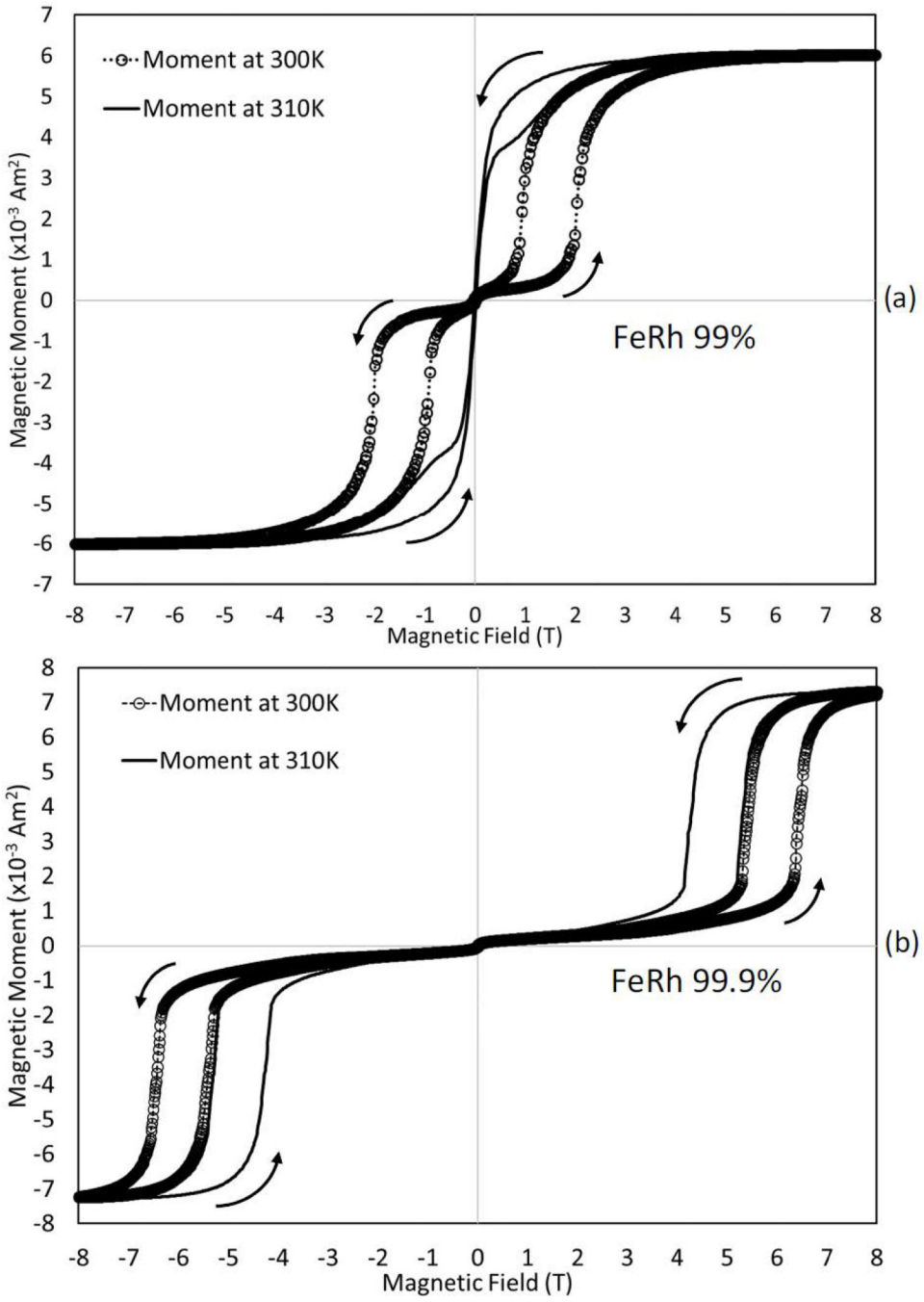

Figure 2.

VSM measurement of Magnetic Moment vs. Magnetic Field of (a) 99% purity Iron-Rhodium (FeRh) disk at temperatures of 27°C (300K) and 37°C (310K) and (b) 99.9% purity FeRh disk at temperatures of 27°C (300K) and 37°C (310K).

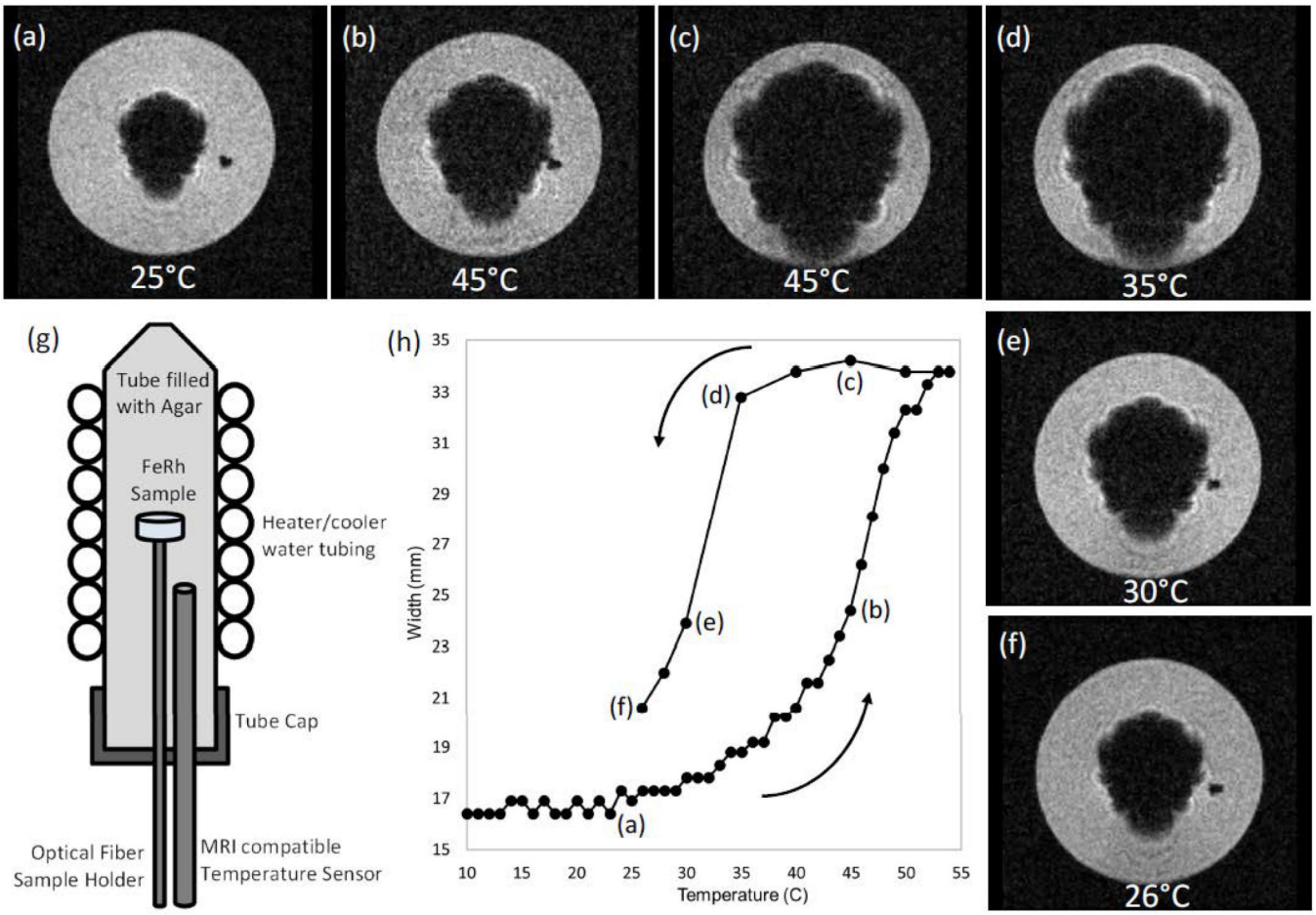

Figure 3.

Temperature dependent MRI images of magneto-caloric FeRh at 4.7T. (a-f) Representative Gradient-echo images through the center of the 99.9% purity FeRh 1mm^3 disk at various temperatures as the sample is heated and then cooled. B_0 is left to right in the images and the stable image feature due to the thermometer next to the sample is on the right side of the image. (g) Diagram of the experimental set-up. (f) Width of the image artifact created by signal loss due to the magnetic field gradients from the FeRh sample as a function of the set-up temperature.

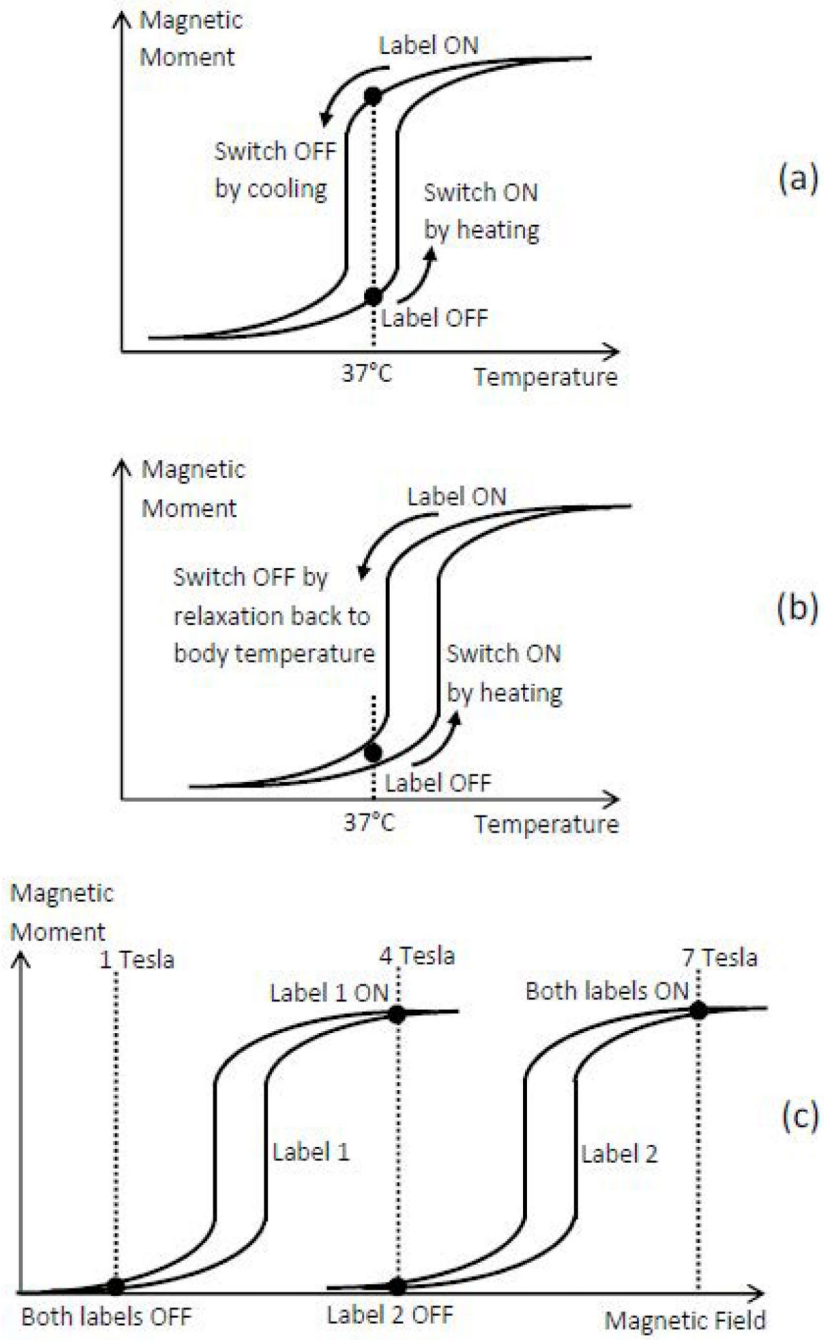

Figure 4.

Magneto-caloric MRI label switching strategies. (a) MRI magnetic field is at the value where the center of the first order magnetic phase transition of the label is at the physiological temperature of 37°C. Temporary heating and cooling switches the label between the MRI visible (ON) and invisible (OFF) states. (b) MRI magnetic field is at the value where the center temperature of the label first order magnetic phase transition is higher than the physiological temperature of 37°C. Temporary heating switches the label to the MRI visible (ON) state while thermal relaxation to equilibrium temperature brings the label

back to the MRI invisible (OFF) state. (c) Multiplexing of two magneto-caloric MRI labels that have phase transitions at two different magnetic field values at the physiological temperature. The two MRI labels are visible or invisible at different magnetic fields and can therefore be differentiated in images from different MRI scanners (in this example at 1T, 4T, and 7T).